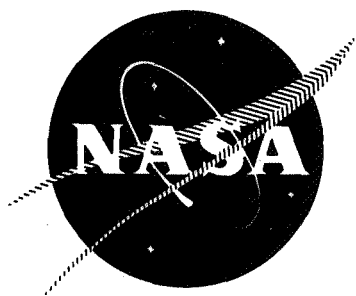TITANIUM PUMP IMPELLER TESTING

FINAL REPORT

by

J. E. Wolf

ROCKETDYNE
A DIVISION OF NORTH AMERICAN ROCKWELL CORPORATION

prepared for

NATIONAL AERONAUTICS AND SPACE ADMINISTRATION
George C. Marshall Space Flight Center
Huntsville, Alabama
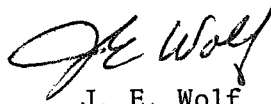
TITANIUM PUMP IMPELLER TESTING

FINAL REPORT

Contract NAS8-25860

Prepared For

National Aeronautics and Space Administration
George C. Marshall Space Flight Center
Huntsville, Alabama

Prepared By

Advanced Systems and Turbomachinery Departments,
Advanced Programs and Engineering
Rocketdyne,
A Division of North American Rockwell Corporation
Canoga Park, California

J. E. Wolf
Principal Engineer
Advanced Turbomachinery

H. G. Diem
Program Manager
Advanced Technology Programs

FOREWORD

Rocketdyne, a Division of North American Rockwell Corporation,
has prepared this final report, which documents the work per-
formed in fulfillment of the program "Titanium Pump Impeller
Testing" during the period 15 June 1970 to 15 December 1970.
This program was sponsored by the National Aeronautics and
Space Administration, Marshall Space Flight Center, Huntsville,
Alabama under Contract NAS8-25860. Mr. Charles Miller, NASA-
MSFC, Huntsville, Alabama, was the Technical Project Manager
for the program.

ABSTRACT

This report describes the Ceramic Stresscoat, burst and pump
testing of two shrouded, diffusion bonded titanium pump impellers.
The Stresscoat test showed a significant decrease in centrifugal
stress in relation to a geometrically similar machined impeller.
The burst test demonstrated a higher tip speed at failure than
the similar machined impeller in spite of an area of poor bonding,
and the liquid hydrogen performance testing demonstrated the practi-
cality of the diffusion bonding process to fabricate shrouded titanium
impellers whose hydrodynamic design is not restricted by current
machining methods.

TABLE OF CONTENTS

LIST OF ILLUSTRATIONS

LIST OF ILLUSTRATIONS

INTRODUCTION

Under a previous contract (NAS8-20761) two diffusion bonded titanium

pump impellers were fabricated to a MK 29 liquid hydrogen pump config-

uration and successfully spin tested to 31,500 rpm.

This program demonstrated the feasibility of the diffusion bonding

process to fabricate shrouded titanium impellers.

To take advantage of this work a follow-on program was undertaken

(Contract NAS8-25860) to further evaluate the diffusion bonding process

by testing. Under this program (a) one impeller was stress coated and

spin tested to determine the magnitude and distribution of the centrif-

ugal stresses, then burst tested to determine the bonded joint efficiency

and (b) the second impeller was installed in a Mark 29F pump assembly and

run under actual pump operating conditions in LH_2 to determine its hydro-

dynamic performance.

SUMMARY

Ceramic Stresscoat, burst and pump testing of the diffusion bonded titanium

impeller has demonstrated the feasibility of its use in a turbopump. The

diffusion bonded design potentially offers higher operating tip speeds

than possible with conventional two piece impellers. The Ceramic Stress

coat test indicated a significant reduction in centrifugal stresses rela-

tive to the geometrically similar, but conventional two piece Mark 29F

machined shrouded impeller assembly. The room temperature burst test

resulted in partial failure of the diffusion bond at 49,000 rpm. The vane tip speed at failure (2560 ft/sec) was higher than that of the Mark 29F impeller assembly which failed at a vane tip speed of 2510 ft/sec. The failure speed ratioed to minimum material properties at the -370 F operating temperature was 52,400 rpm (vane tip speed of 2740 ft/sec).

Three H-Q (head-flow) pump tests, to map impeller performance, were successfully conducted at constant speeds of 12,000, 24,000 and 28,000 rpm. The tests were run at flows ranging from 30% to 135% monimal at 12,000 rpm and 80% to 120% nominal at 24,000 and 28,000 rpm.

DISCUSSION

On initiation of the contract, the two previously fabricated diffusion bonded impellers were removed from the stockroom and impeller #1 (first impeller to be bonded) was selected for use in Task II pump testing and impeller #2 was selected for Task I stress coat and burst testing. The basis for this selection was the premise that, although there was no visual or measurable difference in the two impellers, impeller #2 had the benefit of the assembly, fit up and processing experience gained on impeller #1 and Task I requirements were more severe than Task II.

TASK I - STRESS COAT AND BURST TESTING

Stress Coat Testing

The impeller for Task I was re-inspected and then sent to the machine

shop for minor machining to bring all the necessary dimensions to print

tolerances. Reworking consisted mainly of reducing shroud thickness and

machining to achieve proper radii at the blade inlet and discharge.

Test Procedure

After machining, the impeller was vapor honed to prepare the surface for

the ceramic coating. Because of the complex geometry, spraying techniques

had to be mastered in order to obtain a coating suitable for evaluation.

Many masks were used to prevent overspray from one area to another. After

a suitable spraying technique had been developed, requiring several experi-

ments, the impeller was thoroughly cleaned with AT-201, the ceramic Stress-

coat solvent and the spraying was accomplished. An AT-70 coating was used

with the expectation of achieving a threshold strain of 500 $\mu\epsilon$. After

approximately one-half hour of air drying, the impeller and the calibration

bars were inserted into a furnace, the temperature was slowly increased

(100 F/one-half hour) from ambient to 1025 F, held for 15 minutes, then

slowly ($<$ 40 F/15 minutes) cooled to ambient. After visual examination

indicated a properly glazed coating, the impeller and the calibration bars

were cleaned, then sprayed with Statiflux to determine whether or not any

cracking of the coating had occurred during the glazing operation. It had

not--the coating was suitable for the test. Statiflux is a very fine white powder that is sprayed onto the part through an electrostatic tube. The charged particles are attracted to the base metal where a crack exists in the ceramic coating, thus enabling detection of coating cracks.

After balancing, the part was again checked for coating cracks. It was then spun at a speed lower than that at which cracking would be expected to occur. After each such spin, the impeller was carefully cleaned and inspected for coating cracks, using Statiflux.

Results

There were several spin tests before Stresscoat cracking was observed. The highest was 11,910 rpm, as shown on Table I, along with the subsequent speeds, and the associated stresses and strains. All stresses reported assume a uniaxial plane stress field, the maximum error for this assumption on this hardware being 10% for the lowest stresses and 5% for the highest stresses. The values of stress and strain listed in Table I are those that would exist at the operating speed of 31,000 rpm.

Table II lists the structurally important regions on the impeller in order of decreasing stress, adjusted as the square of the speeds to the operating speed of 31,000 rpm. Photographs of the Stresscoat cracks are included for the more important regions principally to document the direction of the

TABLE I

TEST SPEED (rpm)	THRESHOLD STRAIN AT OPERATING SPEED (b) (10⁻⁶ in./in.)	THRESHOLD STRESS AT OPERATING SPEED (c) (ksi)
11,910(a)	3,520	56.4
12,850	3,030	48.4
13,510	2,740	43.8
14,400	2,410	38.6
15,200	2,160	34.6
16,000	1,950	31.2
16,910	1,750	28.0
17,910	1,560	24.9
19,820	1,270	20.4

Threshold strain for the coating is $520\mu\epsilon$. Elastic modulus of the titanium is 16.0×10^6 psi.

(a) Highest speed at which no cracking of the coating was observed.

(b) The maximum measured principal strain based on plane stress calibration beams and adjusted as the square of the speeds to an operating speed of 31,000 rpm. If the hardware at the boundary of cracking is not in a plane stress state, actual strains are related by the equation $1.06\,\epsilon_x + 0.21\epsilon_y \geq \epsilon_{th}$, where ϵ_x is the maximum principal strain.

(c) The elastically calculated maximum principal stress in a uniaxial plane stress field adjusted as the square of the speeds to an operating speed of 31,000 rpm.

NOTE: The maximum error as a result of the uniaxial plane stress assumption for this hardware is 10% for the lowest stresses and 5% for the highest stresses.

TABLE II

REGIONS WHERE STRESSCOAT CRACKING FIRST OCCURRED

STRESS AT 31,000 Rpm (Ksi)	
48.4	On the vanes at the vane-to-hub radius just back of the leading edge. (Fig. 1, region of cracks, and Fig. 8, the smallest enclosure.)
	On the flat in the upstream hole at the junction of the balance piston holes. (Fig. 3, noted by arrows.)
34.6	On the shroud, both on the flat section and on the radius section. (Fig. 4, regions of cracks, noted by "A" arrows.)
28.0	On the backplate on the radius on both sides of the low pressure balance piston rub ring land. (Fig. 6, noted by "A" arrows.)
24.9	At the vane trailing edge near the shroud. (Fig. 5, region of crack.)
	On the backplate hub between the four balance piston holes and the low pressure balance piston rub ring land. (Fig. 6, noted by "B" arrows.)
	On the flat part of the backplate. (Fig. 6, noted by "C" arrow.)
	In the circumferential groove at the extreme O.D.--indication only. (Fig. 7, region of cracks.)
20.4	On the O.D. of the upper shroud. (Fig. 4, noted by "B" arrow.)
	In the circumferential groove at the extreme O.D. (Fig. 7, region of cracks.)

cracks, for they are aligned perpendicular to the maximum principal stress. The most highly stressed regions are the vanes and the flat in the upstream hole. Figures 1 and 2 illustrate typical vane Stresscoat cracking, initial and extensive, respectively. Figure 3 illustrates the extensive Stresscoat cracking that was first observed in the flat of the upstream hole at 15,200 rpm. Analysis indicated that the Stresscoat in this region first cracked very close to the speed at which first Stresscoat cracking was observed on the vanes, that is, at 12,850 rpm. Figure 4 illustrates the Stresscoat cracking on the shroud. Figure 5 illustrates a vane trailing edge region. Figure 6 illustrates Stresscoat cracking on the backplate, on the flat and on the radii from the low pressure balance piston rub ring land, and also shows some coating loss that occurred at the highest test speed. Figure 7 illustrates Stresscoat cracking that was observed in the circumferential groove at the extreme O.D.

Detailed information was obtained regarding the magnitude, direction, and distribution of stress on the vanes. Figure 8 is a composite average of all seven vanes illustrating the stress boundaries that were observed due to the increasing speed increments, the stress values adjusted as the square of the speeds to an operating speed of 31,000 rpm. The direction of these stresses is normal to the crack pattern, best observed in Fig. 2.

13 510 rpm

Initial Stress Coat Cracking

1CS54-8/6/70-C1E

FIG. 1

Rocketdyne
North American Rockwell
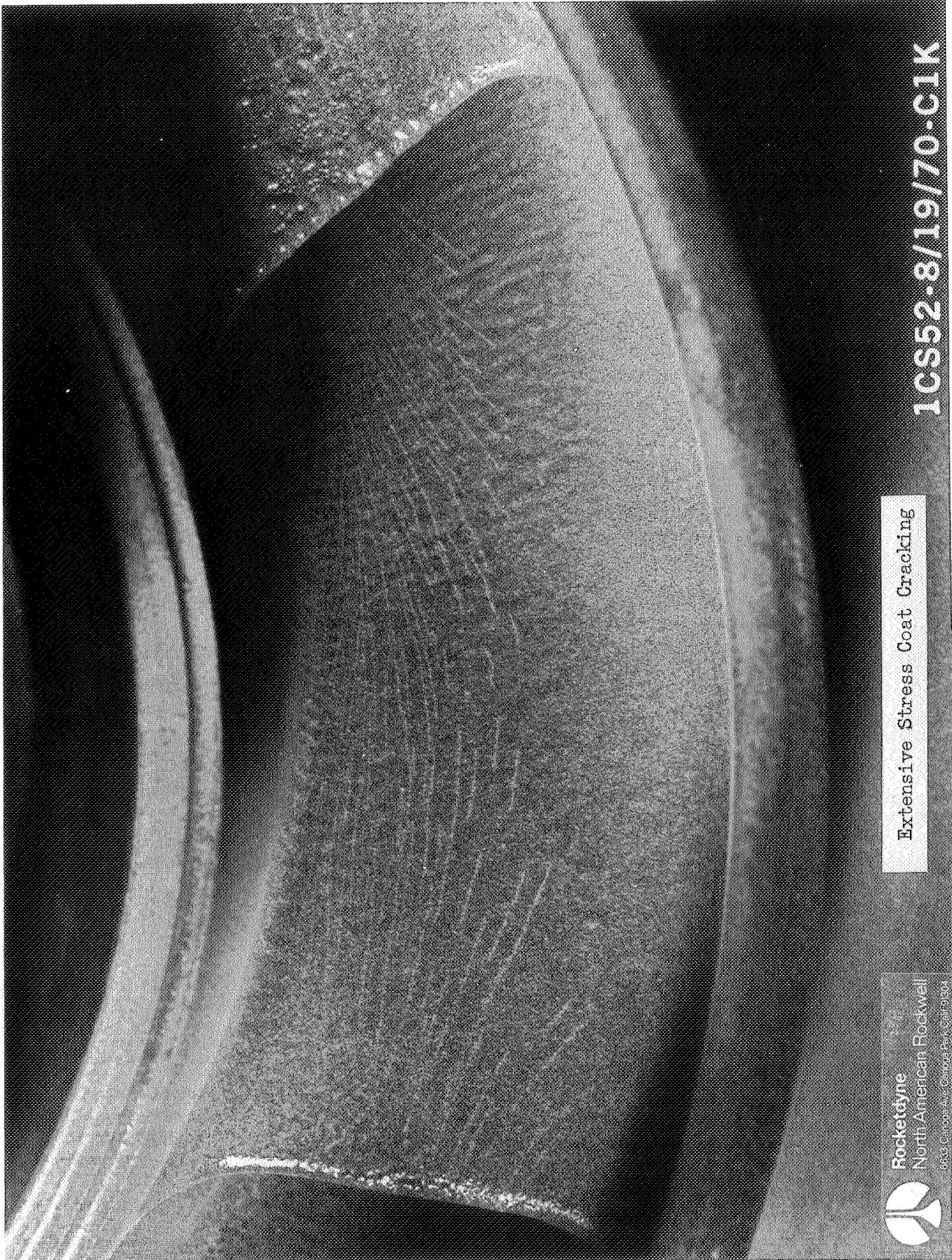
Extensive Stress Coat Cracking

1CS52-8/19/70-C1K

Rocketdyne
North American Rockwell

FIG. 2
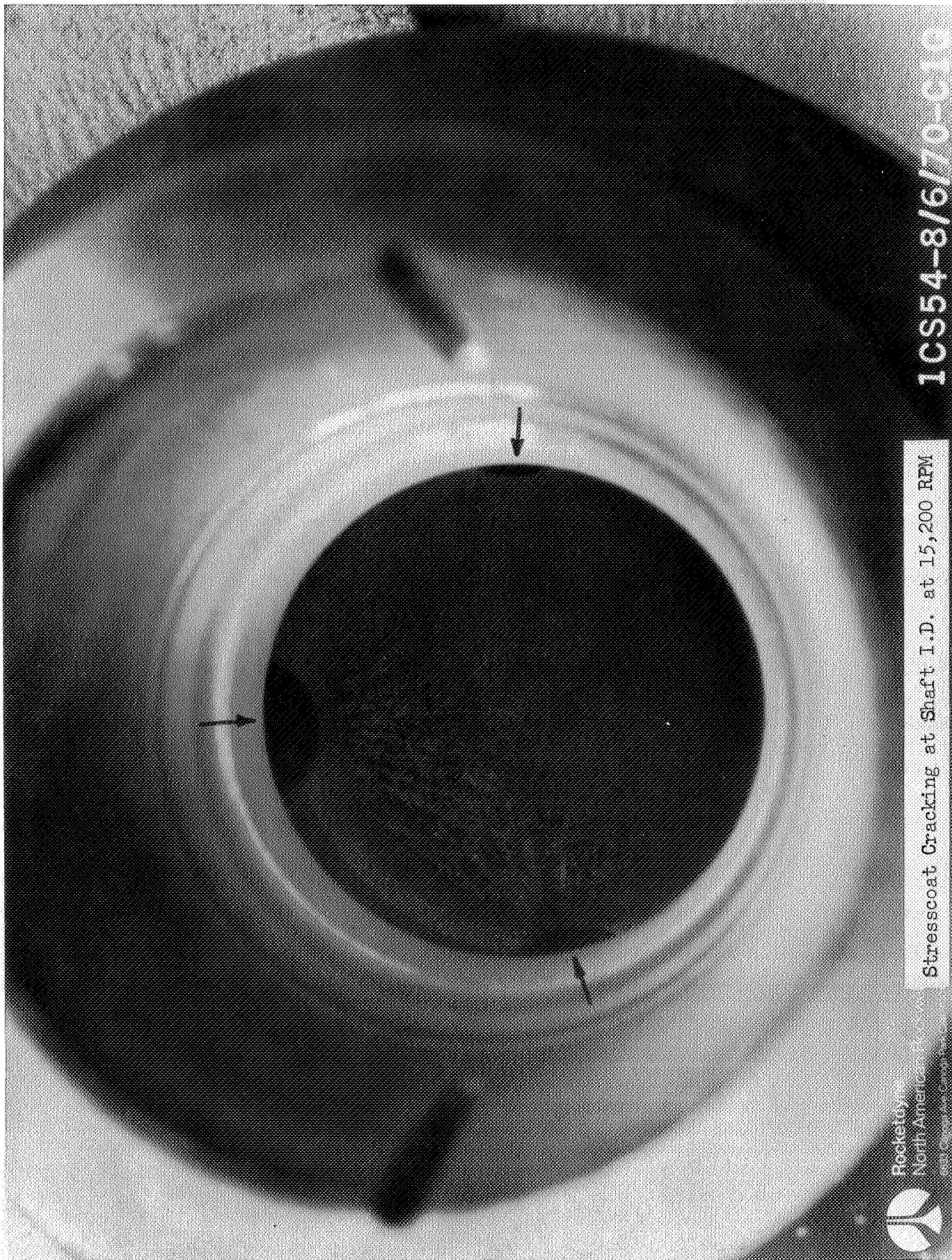
Stresscoat Cracking at Shaft I.D. at 15,200 RPM

1CS54-8/6/70-

FIG. 3
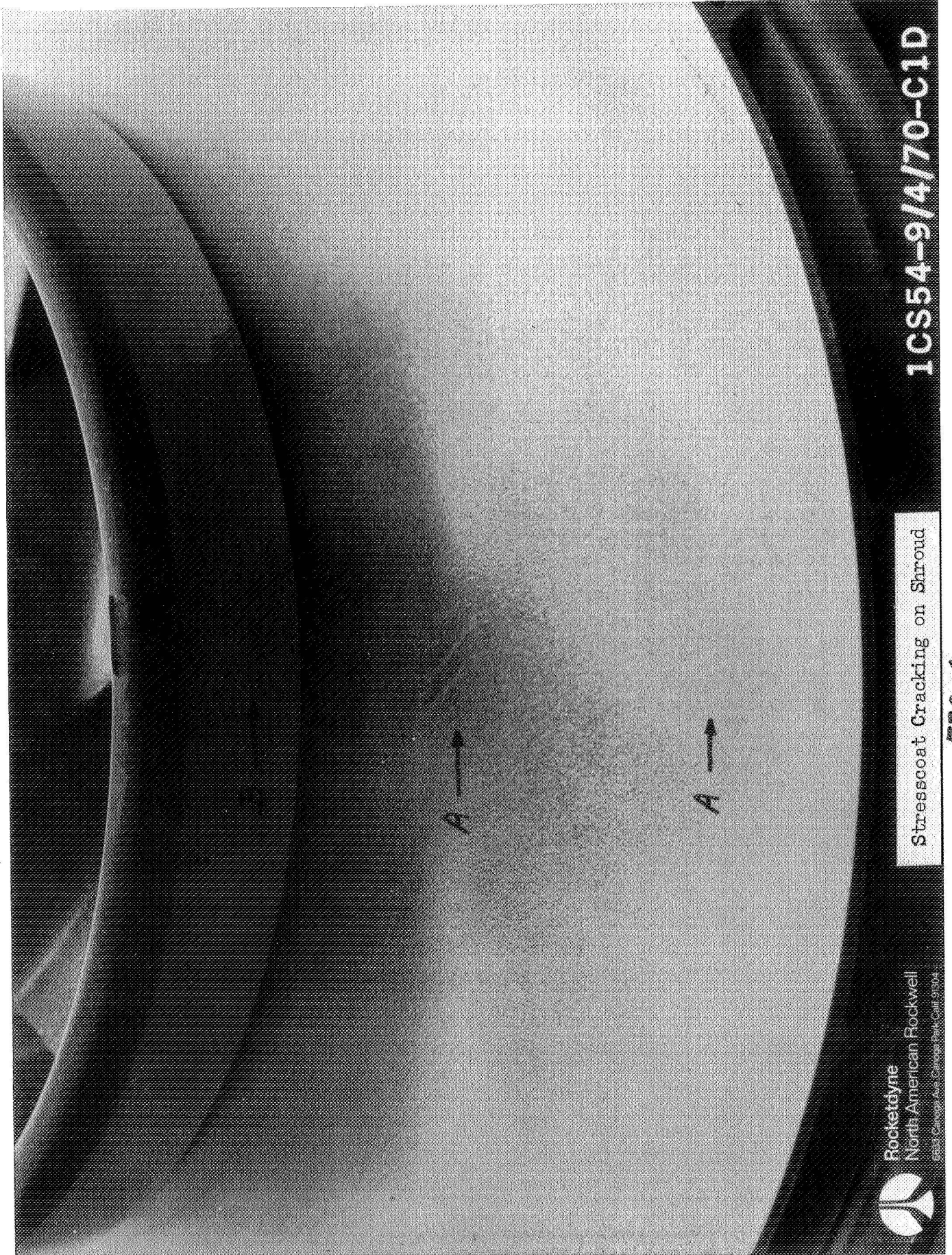
Stresscoat Cracking on Shroud

FIG. 4

1CS54-9/4/70-C1D

Rocketdyne
North American Rockwell
6633 Canoga Ave, Canoga Park, Calif. 91304
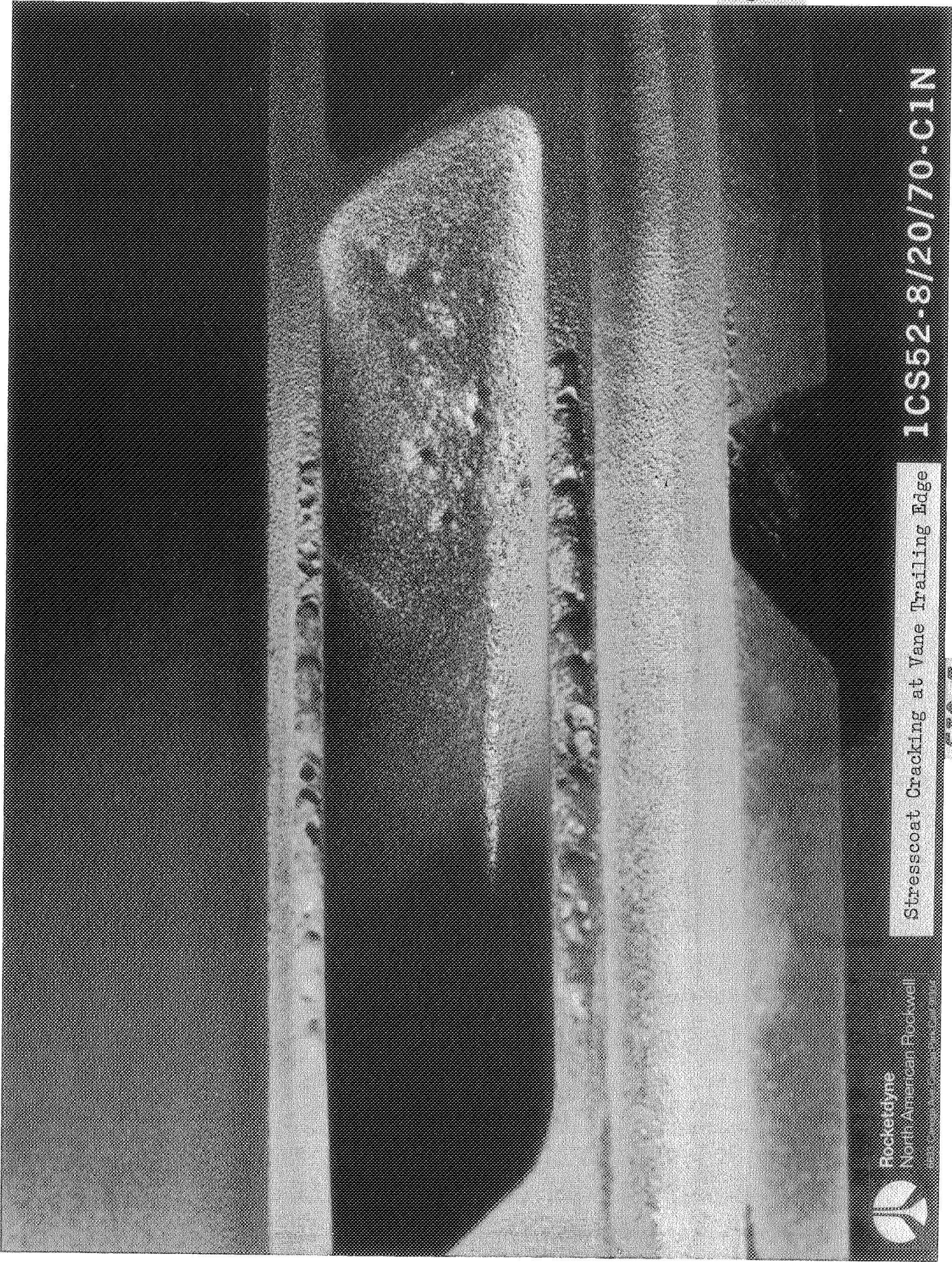
Stresscoat Cracking at Vane Trailing Edge

1CS52-8/20/70-C1N

FIG. 5

Rocketdyne
North American Rockwell
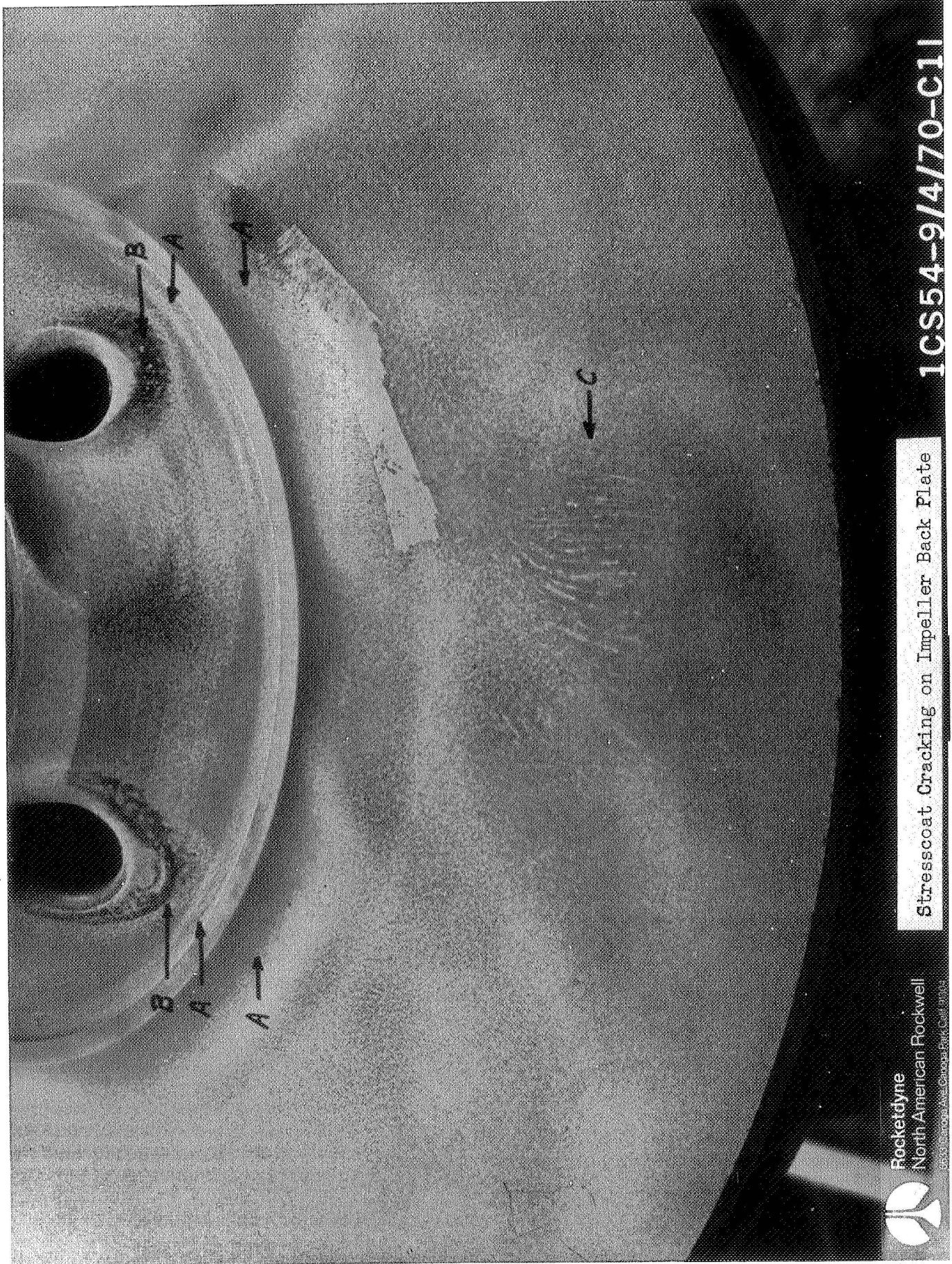
FIG. 6

Stresscoat Cracking on Impeller Back Plate

1CS54-9/4/70-C11

Rocketdyne
North American Rockwell
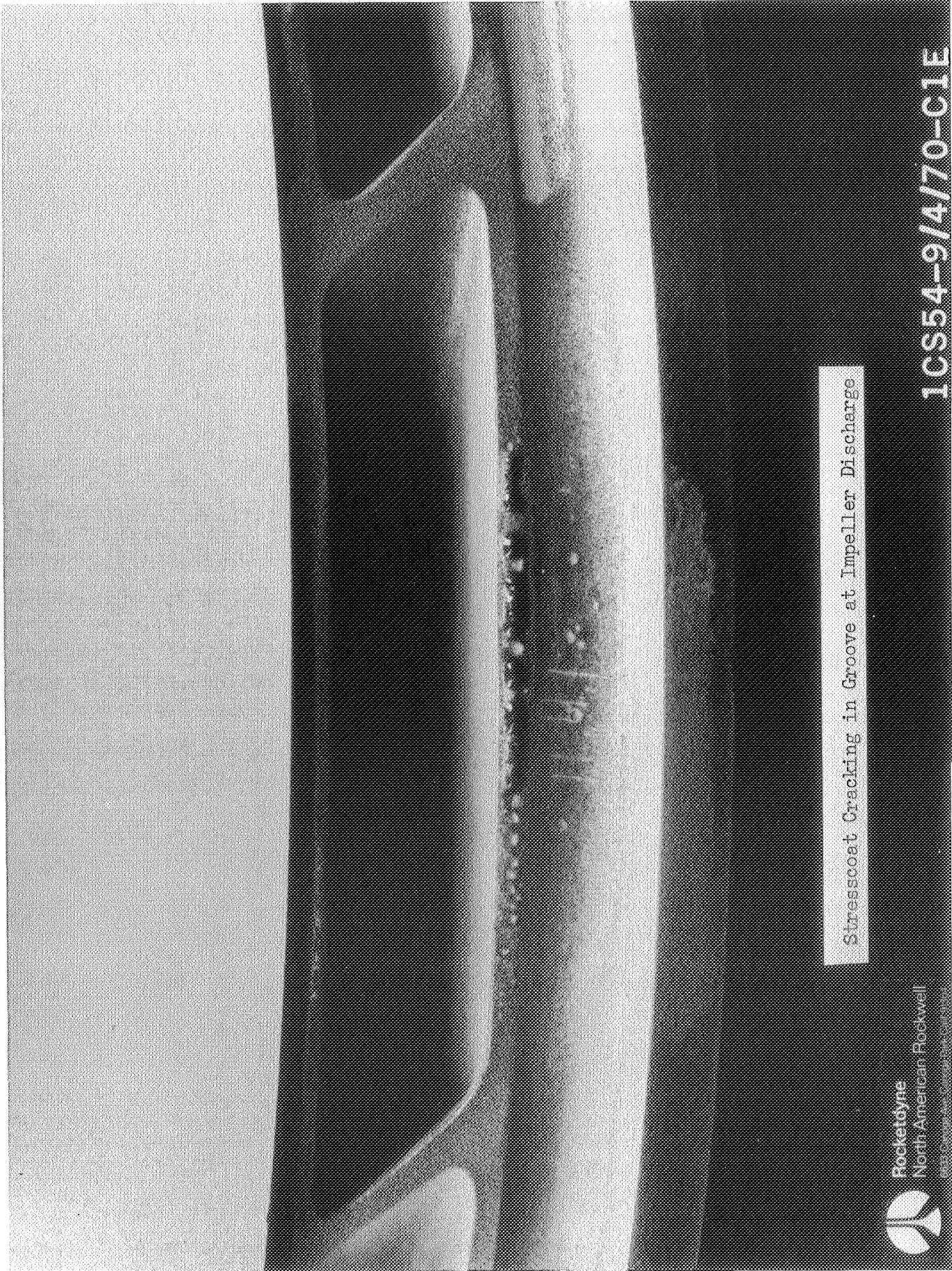
Stresscoat Cracking in Groove at Impeller Discharge

1CS54-9/4/70-C1E

Rocketdyne
North American Rockwell

FIG. 7

MAGNITUDE AND DISTRIBUTION OF VANE STRESSES
ADJUSTED AS THE SQUARE OF THE SPEEDS
TO 31,000 RPM OPERATING SPEED

48.4
43.8
38.6
34.6
31.2
24.9
20.4
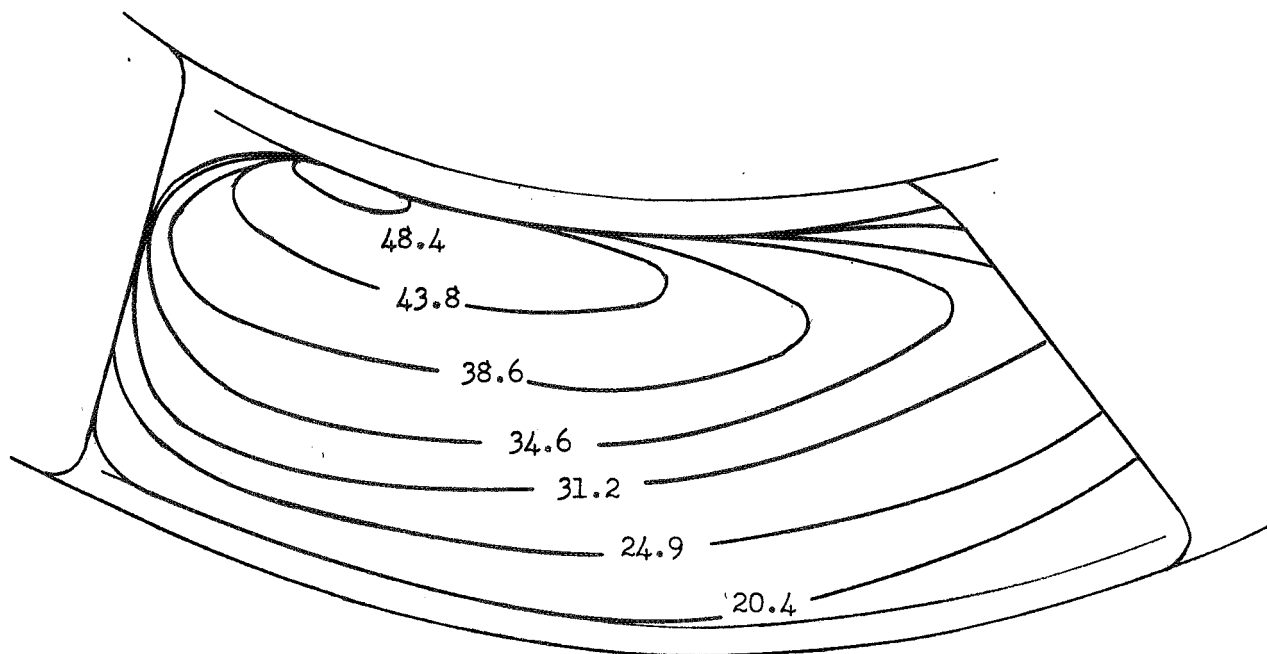
Stress in Ksi

FIGURE 8

Discussion of Results

Of the areas on the impeller that were accessible for coating with Stress-
coat, the most highly stressed would be at one-half of the yield stress at
an operating speed of 31,000 rpm at room temperature.

The coating was "patchy" on both the shroud and the backplate, being either
of proper thickness or too thin. There was enough coverage in each area
for a proper evaluation. The coating in and around the balance piston
holes on the backplate hub was too thick, but the stress was found to be
relatively low in this region. The upstream hole presented major diffi-
culties both in applying the coating and in developing a crack pattern.
Extrapolation was required to properly evaluate this area, because crack-
ing was not observed until it was quite extensive. The downstream hole
was coated too thinly; consequently, an evaluation of that region could
not be made.

The threshold strain values from three bars were within ± 5%, remarkably
close for this type of work. In addition, the impeller contained an area
that could be used for "self-calibration" of the threshold strain. This
was the circumferential groove at the extreme O.D. Using the stress
results from a Rohm & Haas finite element program, there was a minor
crack indication at the second highest speed, which would indicate a
threshold strain somewhat above 480 $\mu\epsilon$. Definite Stresscoat cracking
occurred at the highest speed, Fig. 7, indicating a threshold strain less

than 590 $\mu\epsilon$. Thus, the measured (3 test bars) threshold strain of 520 $\mu\epsilon$ was well bracketed.

As shown in Table II the maximum centrifugal stresses in the impeller vanes when ratioed to the 31,000 rpm operating speed is 48,400 psi. This occurred near the vane leading edge on the suction side at the vane-hub fillet. In comparison, the centrifugal stress at the same location on the two-piece Mark 29F impeller is 77,000 psi. The centrifugal stress in the impeller back plate at comparable locations is 28,000 psi at 31,000 rpm for the diffusion bonded design and 50,400 psi at 31,000 rpm for the Mark 29F impeller assembly. It should be noted that the diffusion bonded impeller and Mark 29F impeller assembly stresscoat test results cannot be directly compared due to different vane geometry. The test results clearly indicate, however, significantly lower centrifugal stresses for the diffusion bonded design. This was anticipated since the one piece diffusion bonded design provides axial continuity through the impeller hub and also more efficient support of the shroud.

Burst Testing

The diffusion bonded impeller was spun in a vacuum at 70 F to failure which occurred at 49,000 rpm, (Vane tip speed of 2560 ft/sec). This corresponds to a failure speed of 59,800 rpm (vane tip speed of 3120 ft/sec) for typical material properties at the -370 F operating temperature and

52,400 rpm (vane tip speed of 2740 ft/sec) for minimum -370 F material
properties.

Figure 9 shows the diffusion bonded impeller mounted in the spin drive
fixture ready to be lowered into the vacuum chamber. Figure 10 shows
the impeller after the burst test at the bottom of the spin pit.

The primary mode of failure was separation of the shroud along the
diffusion bond line in the impeller inlet region as shown in Fig. 11.
The forward portion of the impeller shaft was broken off as a result
of dropping the impeller in the spin pit after the primary failure
occurred.

Examination of the diffusion bond failure indicated regions of poor
bonding as shown in Fig. 12. Magnification of these regions revealed
machining marks on the vanes as shown in Fig. 13. Extrapolation of the
Stresscoat test data indicated that the stress at the failure location
was 51,000 psi at the failure speed. This is well below the parent
material room temperature minimum ultimate strength of 100,000 psi. At
the highest stressed region of the vane, however, (vane to hub junction)
the diffusion bond withstood an equivalent elastic stress of 121,000 psi
as determined from the Stresscoat test data. This strength comparison,
together with the examination of the bond failure, indicates that the
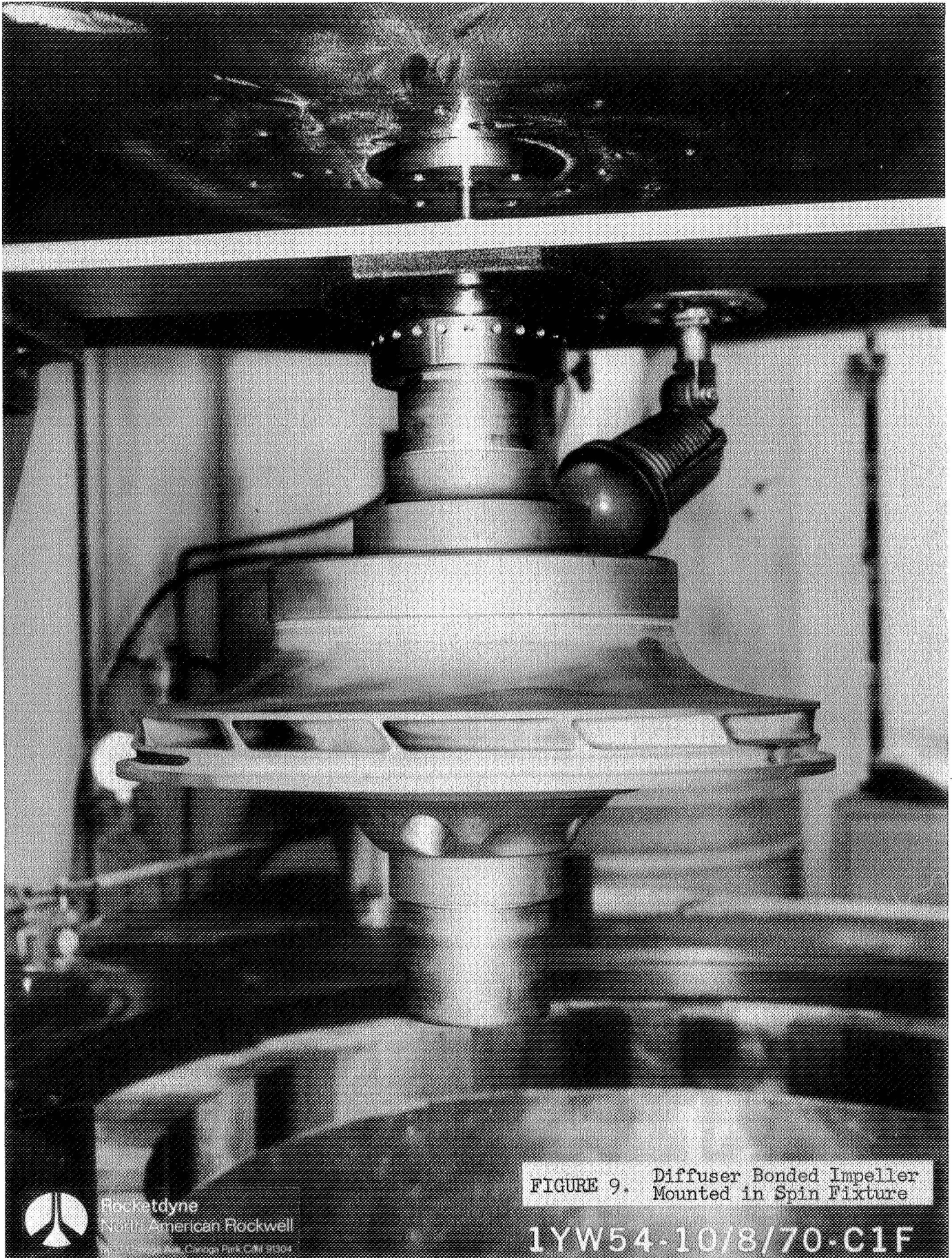
FIGURE 9. Diffuser Bonded Impeller Mounted in Spin Fixture

1YW54-10/8/70-C1F
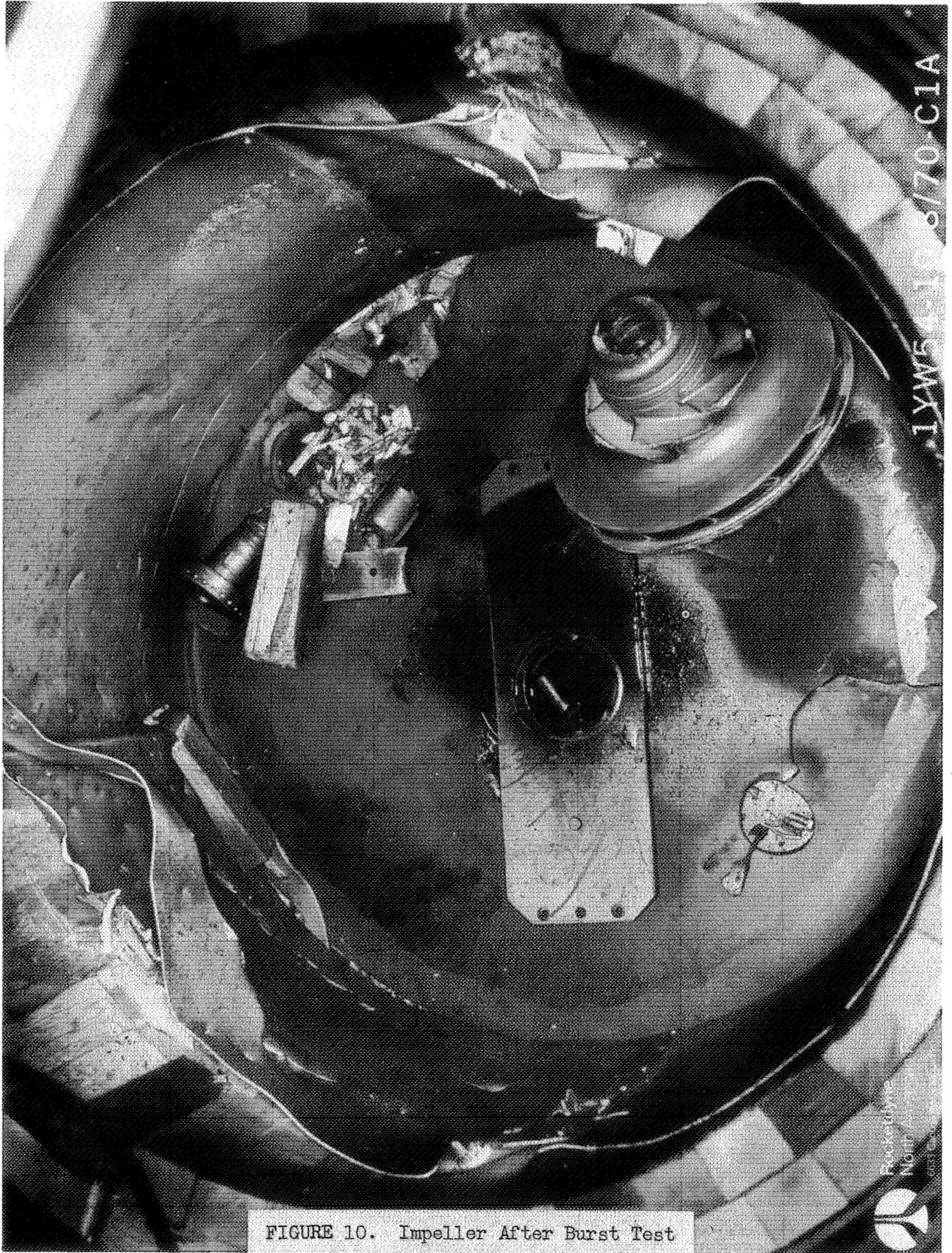
FIGURE 10. Impeller After Burst Test

FIGURE 11. Burst Test Results

1YW54-10/8/70-01B

FIGURE 12. Diffusion Bond Failure

FIGURE 13. 15X Magnification of Machining Marks at Diffusion Bond Failure

1YW54-10/8/70-C1

shroud to vane joint had areas of poor to intermittent bonding. This

condition was not indicated at the bond surfaces by pre-test penetrant

inspection. The imperfect bond would have the same effect as an initial

crack, and would result in premature bond failure.

TASK II - PUMP TESTING

Several changes have been incorporated in the rear bearing journal and

adapter spline areas of the Mark 29F impeller subsequent to the fabri-

cation of the diffusion bonded impeller. In order to permit assembly

of the diffusion bonded impeller into the current Mark 29F pump in a

manner that would allow testing without modifications to the CTL5-3B

test facility, a spacer was fabricated and installed between the end

of the impeller shaft and the splined adapter. This modification affected

only the mechanical linkage; the flow path was not altered. The diffusion

bonded impeller was fabricated with a 12 inch tip diameter in order to

develop the same head at the same rpm with the 37° B_2 as the Mark 29F

impeller (11.5 in tip dia) with a B_2 of 60°. The tip diameter was re-

duced to 11.5 inch to permit installation in the Mark 29 pump. The blade

angle is constant over the zone which was trimmed, hence the discharge

angle was not affected; however, the impeller vane discharge angle is

not matched to the diffuser vane inlet angle and thus additional losses

are to be expected. The information to be gained by designing and fabri-

cating a matched diffuser did not warrant either the cost or time involved.

The H-Q characteristics of the diffusion bonded impeller operating under the above described build conditions were calculated using a modification (based on test data) of the centrifugal pump loss isolation program. The loss isolation program is a computer program developed by Rocketdyne to evaluate the performance of rocket engine centrifugal pumps with a minimum input of design parameters.

The results of this calculation are shown in Fig. 14. Also shown in Fig. 14 is the predicted performance of the Mark 29F impeller and the predicted performance of the diffusion bonded impeller corrected to the 12 inch design diameter. Because of the diffuser mismatch and the difference in the number of vanes between the two impellers, Fig. 14 does not present a true representation of the effects of the reduction in B_2 angle. In order to show the effect of the B_2 parameter calculations were made on a Mark 29F impeller using the loss isolation program and varying only the B_2 angle with a matched diffuser. This data is presented in Fig. 15 and shows H-Q characteristics of (1) a Mark 29F 60° B_2 angle impeller, (2) a Mark 29F impeller with 37° B_2 angle and (3) a Mark 29F impeller with 37° B_2 angle corrected to a 12 inch diameter.

After the diffusion bonded impeller was assembled in the Mark 29F pump, a cross section of which is shown in Fig. 16, the pump was installed in Cell 3B of test facility CTL5.

PREDICTED MK-29F PUMP PERFORMANCE
WITH MARK 29F IMPELLER & DIFFUSION
BONDED TITANIUM IMPELLER USING THE
CENTRIFUGAL PUMP LOSS ISOLATION PROGRAM (MODIFIED)

$N = 28,000$ RPM
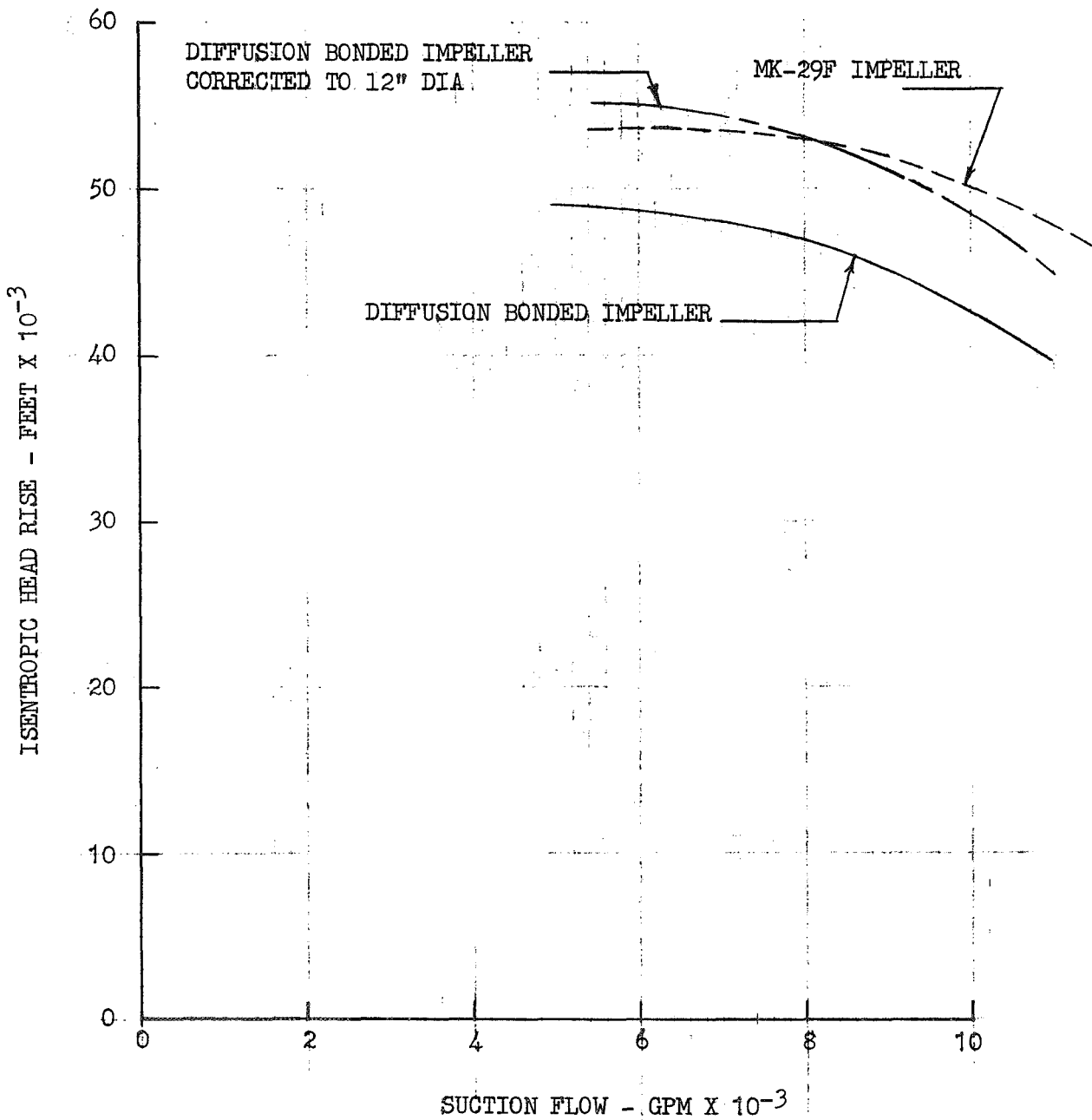
FIGURE 14

PREDICTED MK-29F PUMP PERFORMANCE
USING THE CENTRIFUGAL PUMP LOSS
ISOLATION PROGRAM

37° IMPELLER DISCHARGE BLADE
ANGLE CORRECTED TO 12 INCH DIA.

60° IMPELLER DISCHARGE
BLADE ANGLE

37° IMPELLER DISCHARGE
BLADE ANGLE

HEAD - FEET X 10^3

FLOW - GPM X 10^-3
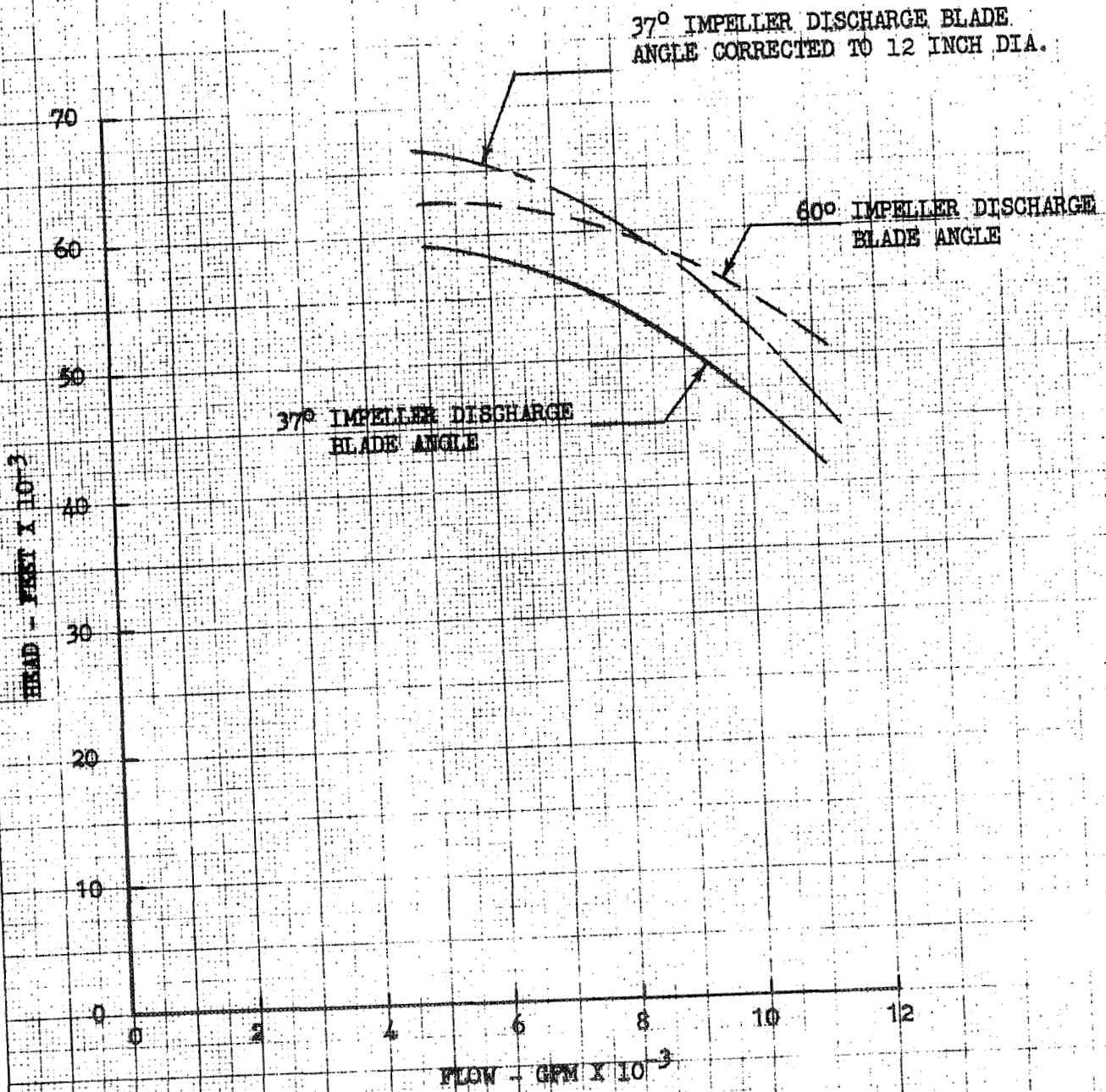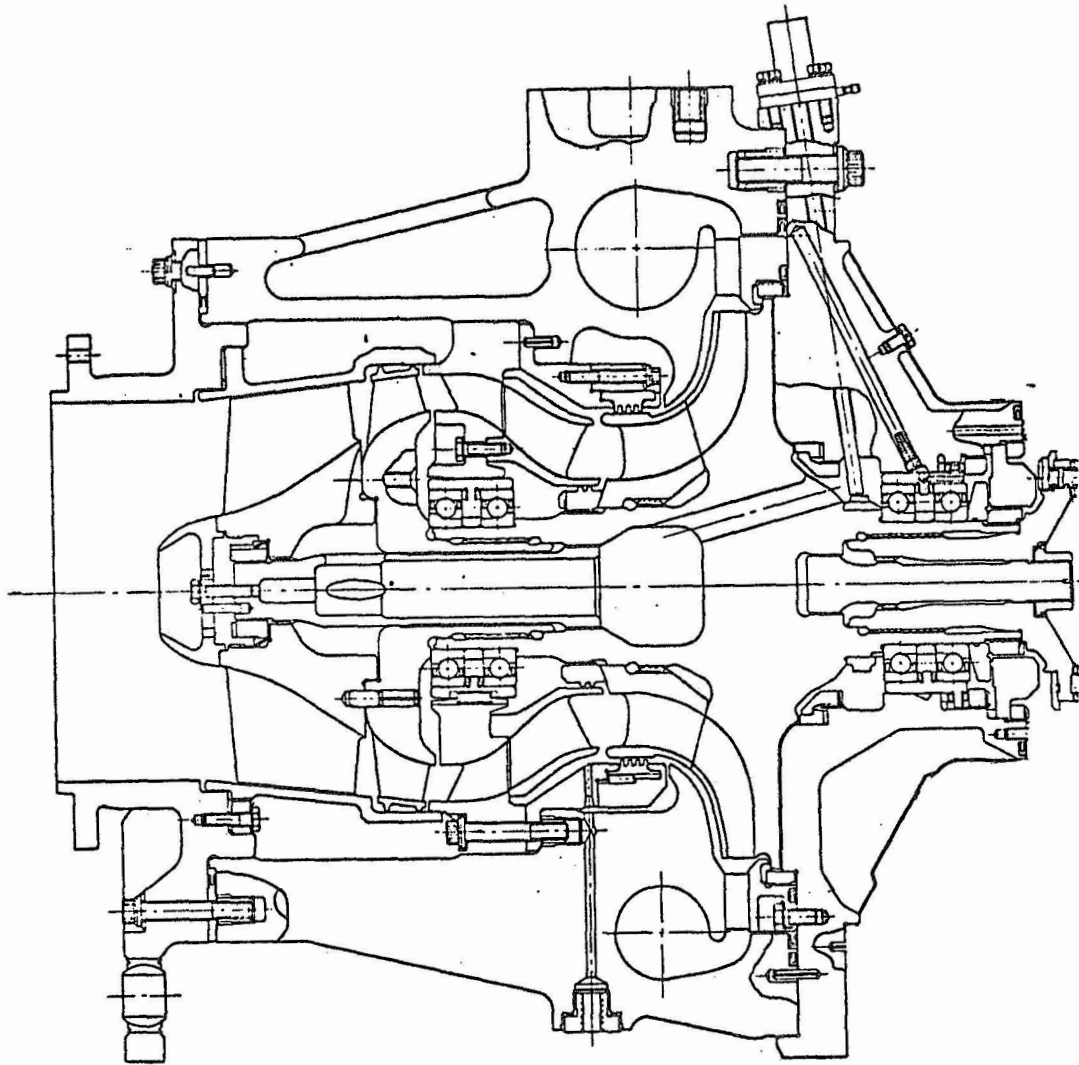
FIGURE 15

MK-29 FUEL PUMP

FIGURE 16

Cell 3B is shown in Fig. 17 and the cell flow circuit is shown in Fig. 18.
The circuit includes two 20,000 gallon, 110 psi tanks. For extended opera-
tion, the flow mode is from the run tank through 10 inch vacuum-jacketed
lines to the pump. The fluid returns by 10 inch ducting and flows to a
heat exchanger in the catch tank (boil off is vented to a stack) and is
then returned to the run tank. To minimize tanking interference an off-
site fill point is plumbed to a 45,000 gallon liquid hydrogen storage
vessel. Electric drive power is supplied by a variable speed, synchronous
motor generator drive system of 17,500 horsepower. This system drives the
Cell 3B gear box.

Mark 29 fuel pump S/N R004-2 with the diffusion bonded impeller is shown
installed in Cell 3B in Fig. 19 and 20.

Test Procedure

Performance of the diffusion bonded impeller was determined by conducting
three H-Q tests at constant speeds of 12,000, 24,000 and 28,000 rpm. Tests
were conducted at flows ranging from 30% to 135% of nominal at 12,000 rpm
and 80% to 120% of nominal at 24,000 and 28,000 rpm.

Specific test points were as follows:

Test #1

At 24,000 rpm the following flows were held for a minimum of
5 seconds each: 6,750 (80% nom.), 8,435 (nominal) and 10,120
(120% nom.).
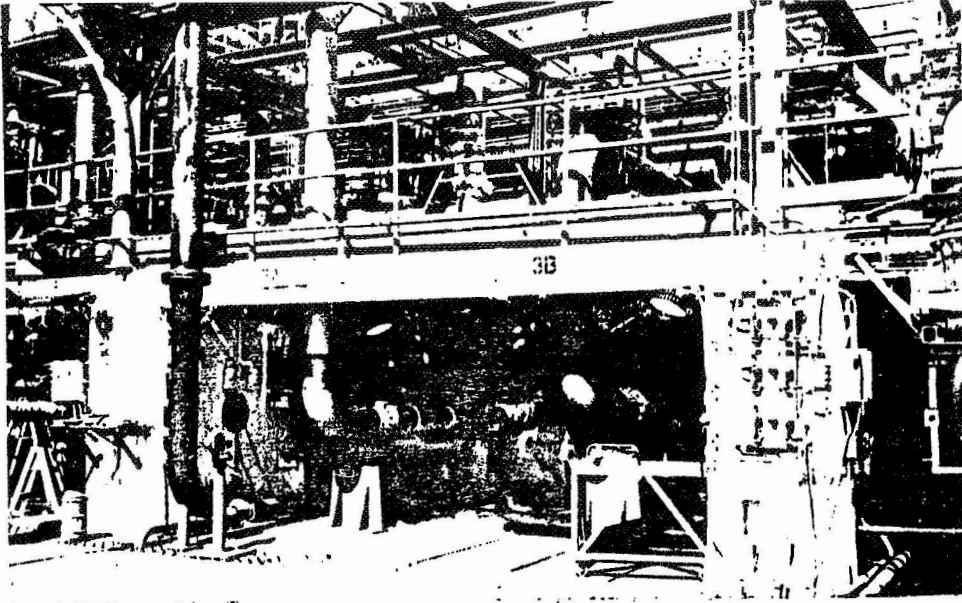
Figure 17. Liquid Hydrogen Pump Test Cell-3B at CTL-5
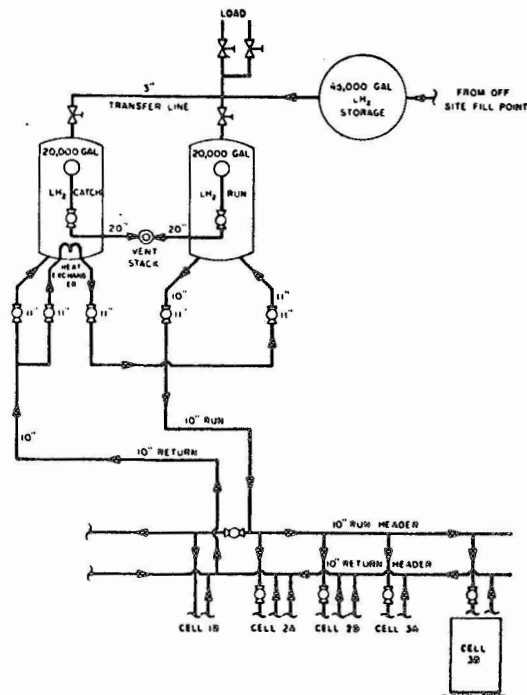
Figure 18. CTL-5 Liquid Hydrogen Flow
Circuit
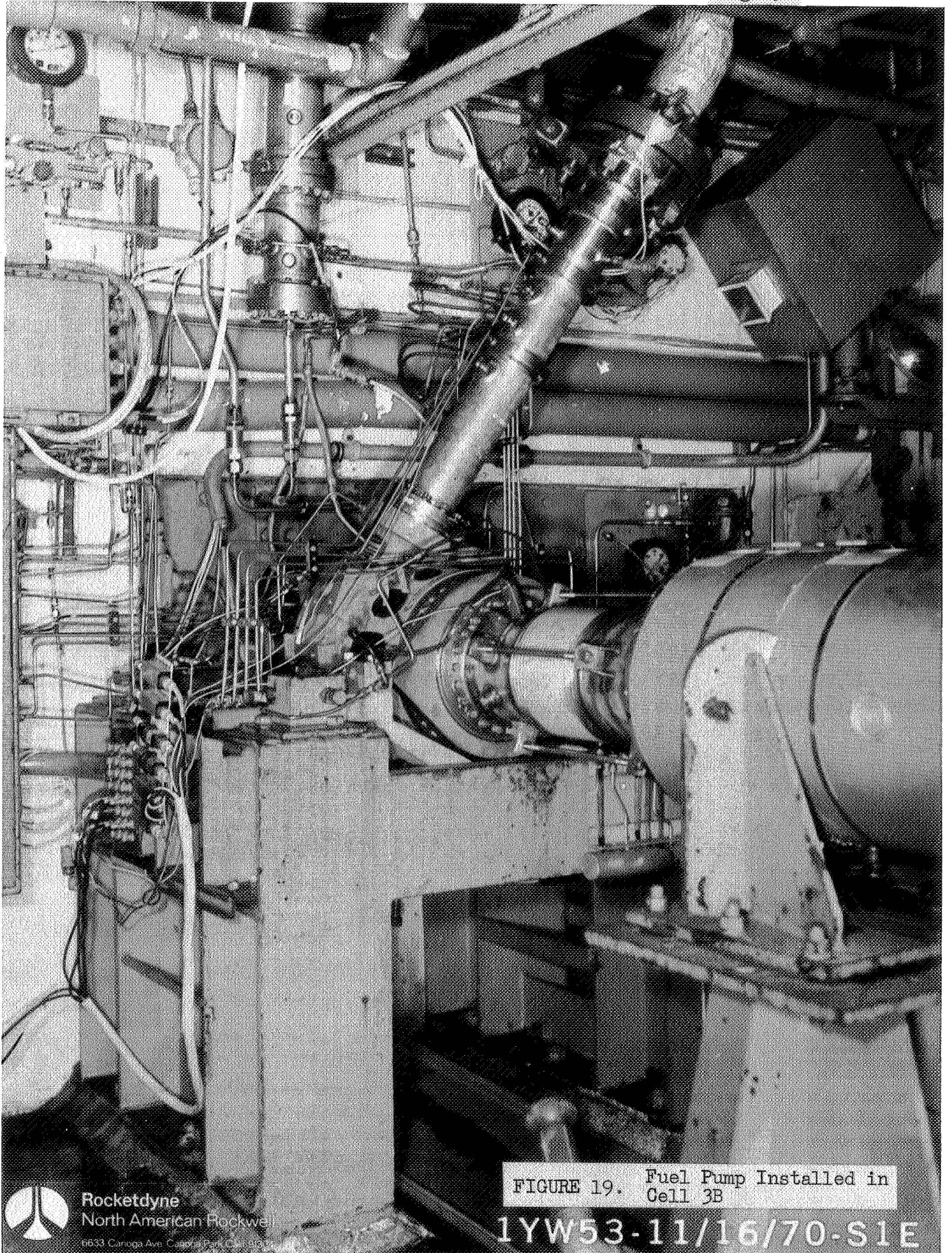
FIGURE 19. Fuel Pump Installed in Cell 3B

1YW53-11/16/70-S1E

Rocketdyne
North American Rockwell
6633 Canoga Ave. Canoga Park Cali 91304

Page 32
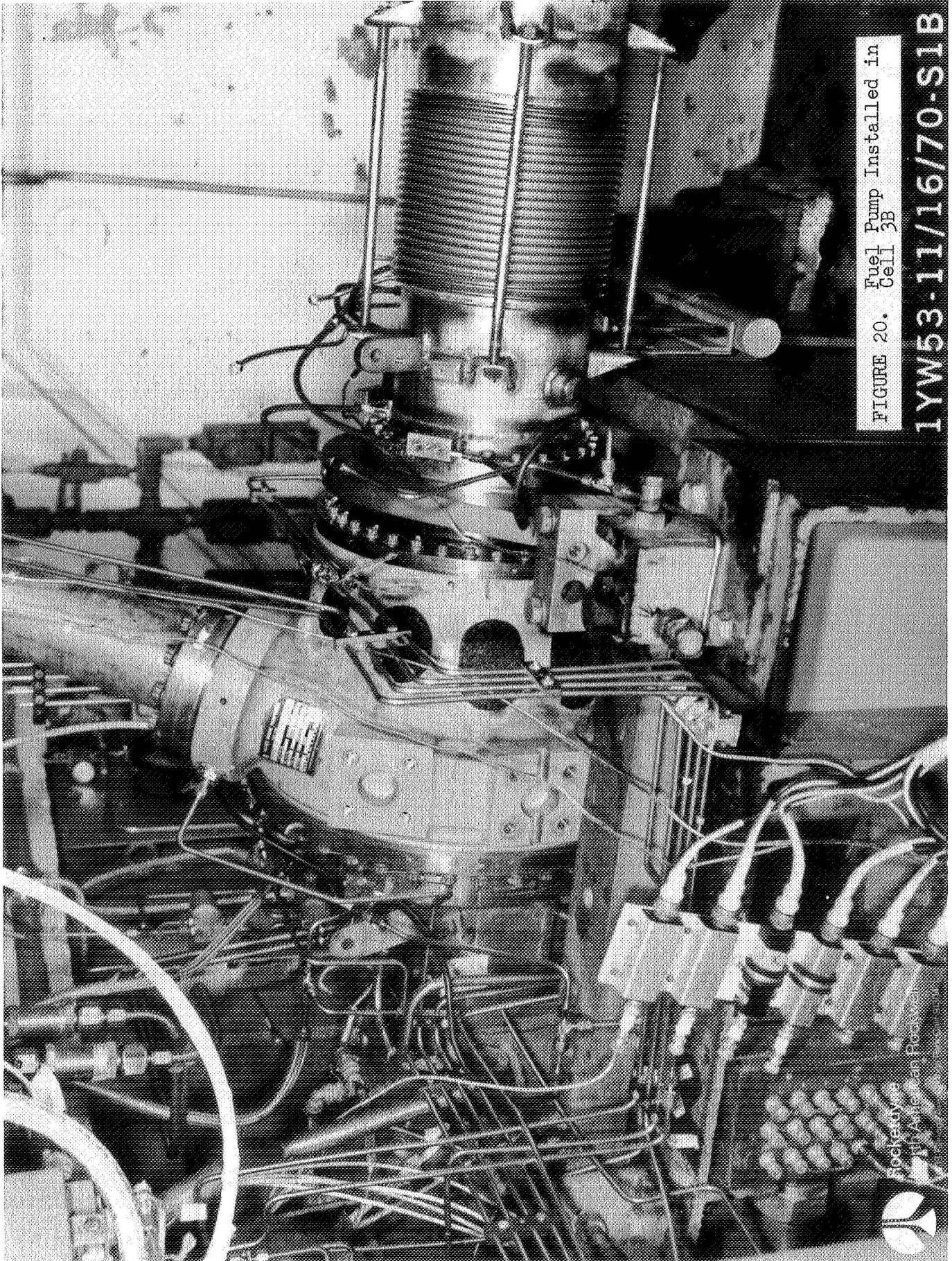
FIGURE 20. Fuel Pump Installed in Cell 3B

1YW53-11/16/70-S1B

Test #2

At 28,000 rpm the following flows were held for a minimum of
5 seconds: 7,850 (80% nom.), 9,810 (nominal) and 11,772
(120% nom.).

Test #3

At 12,000 rpm the following flows were held for a minimum of
5 seconds: 1,265 (30% nom.), 1,690 (40% nom.), 2,110 (50% nom.),
2,530 (60% nom.), 2,955 (70% nom.), 3,375 (80% nom.), 3,800 (90%
nom.), 4,220 (nominal), 4,640 (110% nom.), 5,065 (120% nom.),
5,485 (130% nom.), 5,910 (140% nom.), and 6,330 (150% nom.).

For each of the above test points double excursions were performed.

Results

Test results are plotted in Fig. 21, 22 and 23. Figure 21 shows the
isentropic head rise as a function of flow which agrees quite closely
with the predicted performance as shown in Fig. 14. The measured head
is slightly lower than predicted at all flows which indicates the losses
produced by the mismatch between the diffusion bonded impeller and the
stationary elements of the Mark 29F pump are greater than predicted.

Figure 22 shows the pump isentropic efficiency as a function of suction
flow and Fig. 23 shows head coefficient and isentropic efficiency as a
function of flow coefficient. Similar data from testing a previous build
of pump No. R004 are also shown on each figure for comparison.

MARK 29 FUEL PUMP PERFORMANCE
WITH DIFFUSION BONDED TITANIUM
IMPELLER BASED ON TESTS OF PUMP
S/N R004-2
COMPARED WITH
MARK 29F PUMP PERFORMANCE WITH
STANDARD MARK 29F IMPELLER (R004-1)
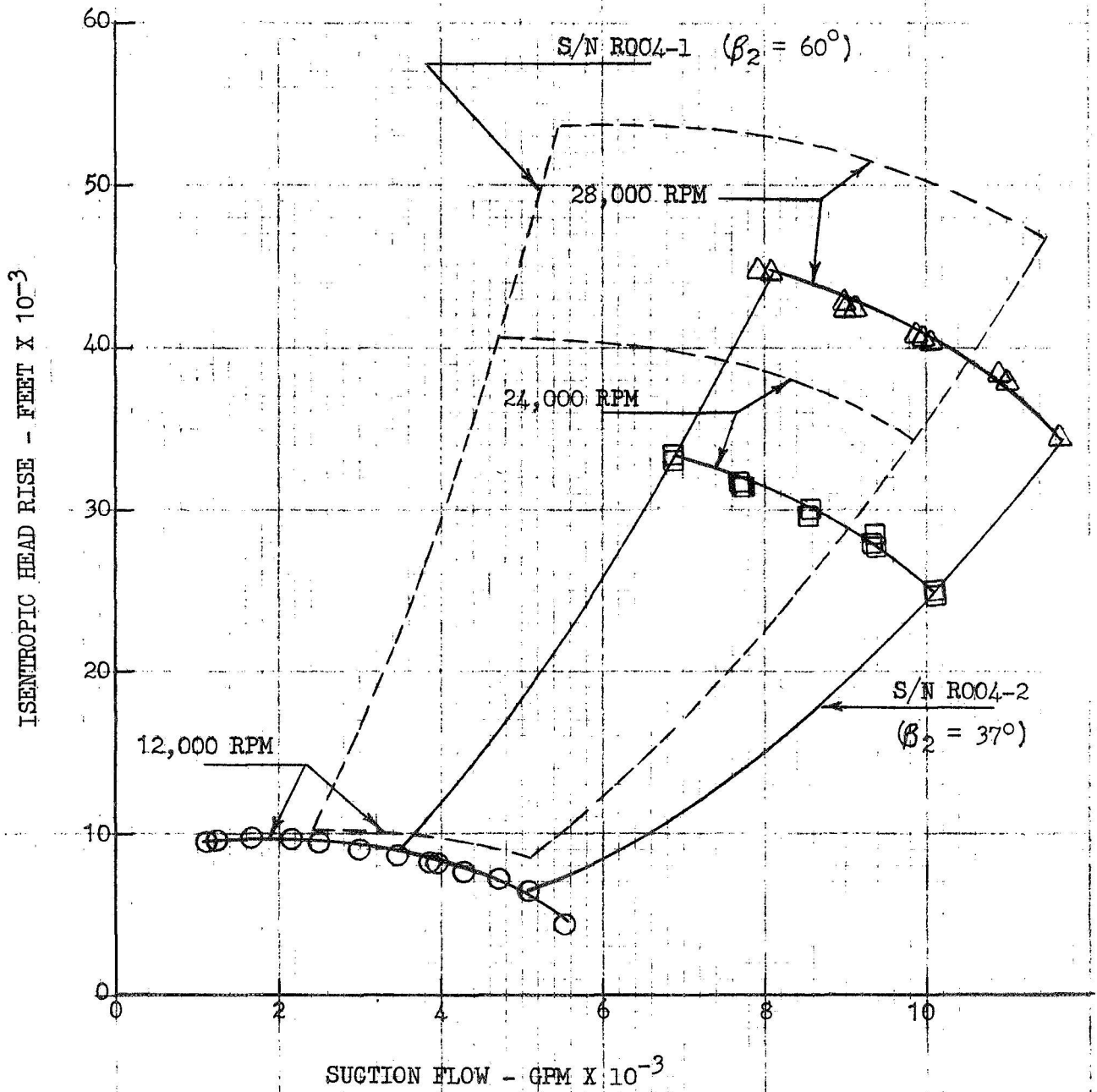
FIGURE 21

MARK 29 FUEL PUMP EFFICIENCY WITH
DIFFUSION BONDED TITANIUM IMPELLER (R004-2)
AND STANDARD MARK 29F IMPELLER (R004-1)

R004-1 $(\beta_2 = 60°)$
R004-2 $(\beta_2 = 37°)$

28,000 RPM

24,000 RPM

ISENTROPIC EFFICIENCY = %

SUCTION FLOW – GPM X 10^{-3}
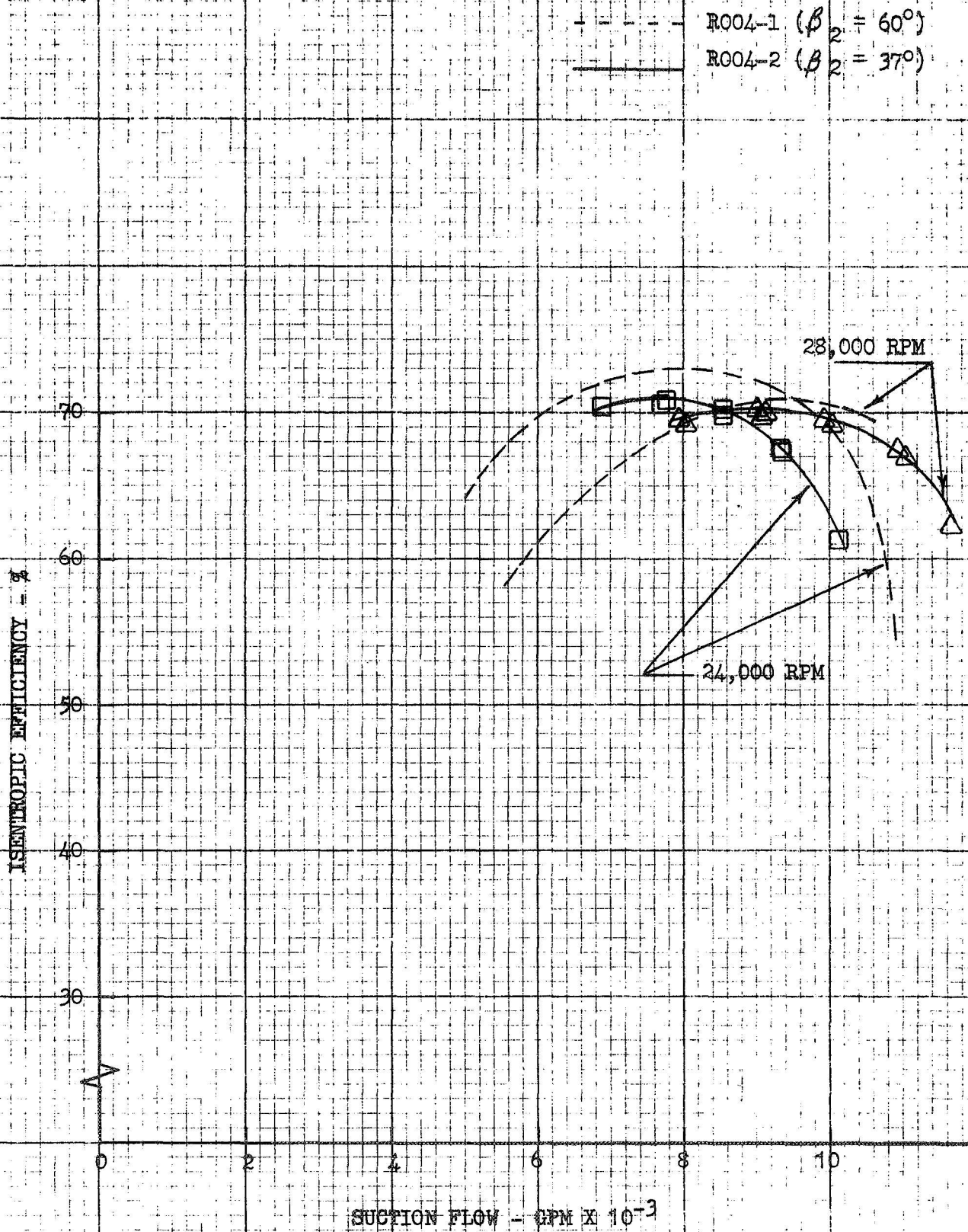
FIGURE 22

MARK 29 FUEL PUMP PERFORMANCE WITH
DIFFUSION BONDED TITANIUM IMPELLER (R004-2)
AND STANDARD MARK 29F IMPELLER (R004-1)
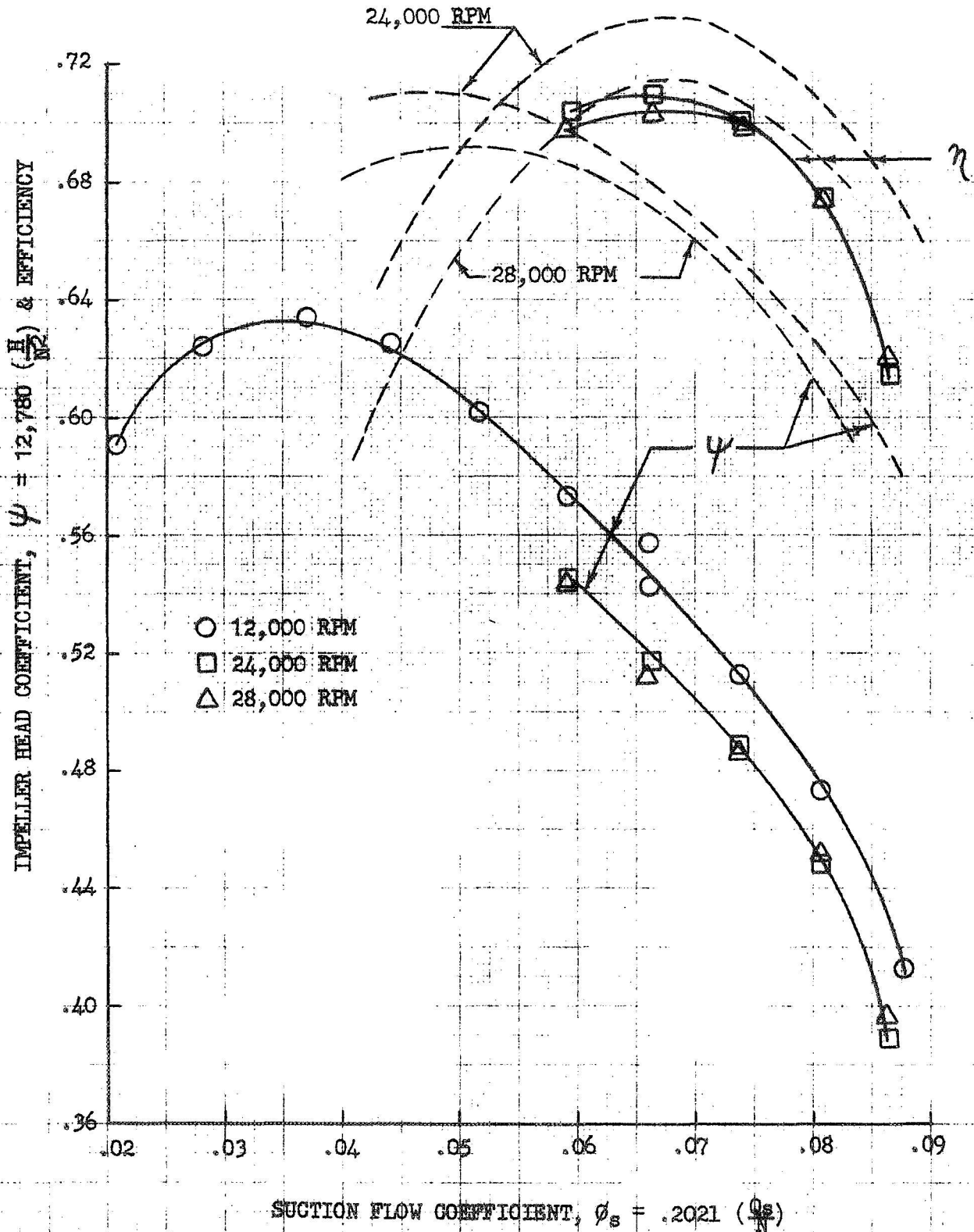
FIGURE 23

CONCLUSIONS

1. The ceramic stress coat testing indicated a significant reduction
   in centrifugal stresses relative to the geometrically similar two
   piece machined Mark 29F shrouded impeller assembly.

2. The room temperature burst test resulted in a partial failure of the
   diffusion bond at 49,000 rpm. Despite the bond failure the vane tip
   speed at failure (2,560 ft/sec) was higher than that of the Mark 29F
   impeller assembly which failed at a vane tip speed of 2,510 ft/sec.

   The room temperature failure corresponds to a failure speed of 59,800
   rpm (vane tip speed of 3,120 ft/sec) for typical material properties
   at the -370 F operating temperature.

3. The measured H-Q performance of the diffusion bonded titanium impeller
   shows good agreement with predicted performance and demonstrates the
   practicality of this method of fabrication which allows shrouded
   titanium impellers to be fabricated based on hydrodynamic considera-
   tions instead of being limited by maching methods.

4. In the area of the bond failure, it is difficult to apply radial
   pressure to the mating parts during the bonding process. In this
   area the applied pressure is at least partially reacted by the hoop
   strength of the shroud. During the bonding process the shroud was

much thicker than in its final configuration. Since sufficient

pressure must be applied to overcome the hoop strength of the shroud

in order to produce the desired pressure at the vane-shroud joint,

consideration should be given to decreasing the shroud thickness

at the time of the bonding. Particular attention should be given

to the fit and surface finish of the mating parts in the area of

the bond failure due to this difficulty.

DISTRIBUTION LIST FOR FINAL TECHNICAL REPORT
CONTRACT NAS8-25860

Copies	Recipient	Designee
	NASA Headquarters Washington, D. C. 20546	
1	Contracting Officer	X
	NASA-Lewis Research Center 21000 Brookpark Road Cleveland, Ohio 44135	
1	Office of Technical Information	X
	NASA-Manned Spacecraft Center Houston, Texas 77001	
	Office of Technical Information	X
	NASA-Marshall Space Flight Center Huntsville, Alabama 35812	
2	Office of Technical Information, MS-IP	X
1	Technical Library	X
1	Dale Burrows, S&E-ASTN-PJ	X
	Jet Propulsion Laboratory 4800 Oak Grove Drive Pasadena, California 91103	
2	Louis Toth	X
3	Chief, Liquid Propulsion Technology, RPL Office of Advanced Research and Technology NASA Headquarters Washington, D. C. 25046	X
1	Director, Technology Utilization Division Office of Technology Utilization NASA Headquarters Washington, D. C. 20546	X
20	NASA Scientific and Technical Information Facility P. O. Box 33 College Park, Maryland 20740	X

Copies	Recipient	Designee
1	Director, Launch Vehicles and Propulsion, SV Office of Space Science and Applications NASA Headquarters Washington, D. C. 20546	X
1	Director, Advanced Manned Missions, MT Office of Manned Space Flight NASA Headquarters Washington, D. C. 20546	X
1	NASA Pasadena Office 4800 Oak Grove Drive Pasadena, California 91103 Patents and Contracts Management	X
1	Jet Propulsion Laboratory 4800 Oak Grove Drive Pasadena, California 91103 D. D. Lawson, Technical Monitor	X

NASA Field Centers

Copies	Recipient	Designee
1	Ames Research Center Moffett Field, California 94035	Hans M. Mark
1	Goddard Space Flight Center Greenbelt, Maryland 20771	Merland L. Mosenson Code 620
2	Jet Propulsion Laboratory California Institute of Technology 4800 Oak Grove Drive Pasadena, California 91103	Henry Burlage, Jr. Propulsion Div. 38
1	Langley Research Center Langley Station Hampton, Virginia 23365	Ed Cortwright Director
1	Lewis Research Center 21000 Brookpark Road Cleveland, Ohio 44135	Director

Copies	Recipient	Designee
1	Marshall Space Flight Center Huntsville, Alabama 35812	Hans G. Paul S&E-ASTN-P, Bldg. 4666
1	Manned Spacecraft Center Houston, Texas 77001	J. G. Thibodaux, Jr. Chief, Prop. & Power Div.
1	John F. Kennedy Space Center, NASA Cocoa Beach, Florida 32931	Dr. Kurt H. Debus

Government Installations

Copies	Recipient	Designee
1	Air Force Missile Test Center Patrick Air Force Base, Florida	L. J. Ullian
1	Space and Missile Systems Organization Air Force Unit Post Office Los Angeles, California 90045	Colonel Clark Technical Data Center
1	Arnold Engineering Development Center Arnold Air Force Station Tullahoma, Tennessee 37383	Dr. H. K. Doetsch
1	Bureau of Naval Weapons Department of the Navy Washington, D. C. 20546	J. Kay RTMS-41
1	Defense Documentation Center Headquarters Cameron Station, Building 5 5010 Duke Street Alexandria, Virginia 22314 Attn: TISIA	
1	Headquarters, U. S. Air Force/Pentagon Washington, D. C. 20546 Attn: AFRDD	
1	Picatinny Arsenal Dover, New Jersey 07801	T. Forsten, Chief Liquid Propulsion Lab

Copies	Recipient	Designee
1	Air Force Rocket Propulsion Laboratory Research and Technology Division Air Force Systems Command Edwards, California 93523	RPRPD/Mr. H. Main
1	U.S. Army Missile Command Redstone Arsenal Alabama 35809	Dr. Walter Wharton
1	U.S. Naval Ordnance Test Station China Lake, California 93557	CODE 4562 Chief, Missile Propulsion Division
1	Wright-Patterson Air Force Base Ohio 45433	AFML (MANC D. L. Schmidt)

CPIA

1	Chemical Propulsion Information Agency Applied Physics Laboratory 8621 Georgia Avenue Silver Spring, Maryland 20910	Tom Reedy

Industry Contractors

1	Aerojet-General Corporation P. O. Box 296 Azusa, California 91703	W. L. Rogers
1	Aerojet-General Corporation P. O. Box 1947 Technology Library, Bldg. 2015, Dept. 2410 Sacramento, California 95809	R. Stiff
1	Space Division Aerojet-General Corporation 9200 East Flair Drive El Monte, California	S. Machlawski
1	Aerospace Corporation 2400 East El Segundo Boulevard P. O. Box 95085 Los Angeles, California 90045	John G. Wilder MS-2293

Copies	Recipient	Designee
1	Atlantic Research Company Edsall Road and Shirley Highway Alexandria, Virginia 22314	Dr. Ray Friedman
1	Avco Systems Division Wilmington, Massachusetts	Howard B. Winkler
1	Beech Aircraft Corporation Boulder Division Box 631 Boulder, Colorado 80302	J. H. Rodgers
1	Bell Aerosystems Company P. O. Box 1 Buffalo, New York 14240	W. M. Smith
1	Bellcomm 955 L'Enfant Plaza Washington, D. C. 20024	H. S. London
1	Bendix Systems Division Bendix Corporation 3300 Plymouth Road Ann Arbor, Michigan 48105	John M. Brueger
1	Boeing Company P. O. Box 3707 Seattle, Washington 98124	J. D. Alexander W. W. Kann
1	Boeing Company 1625 K Street, N.W. Washington, D. C. 20006	Library
1	Missile Division Chrysler Corporation P. O. Box 2628 Detroit, Michigan 48231	John Gates
1	Wright Aeronautical Division Curtis-Wright Corporation Woodridge, New Jersey 07075	G. Kelley

Copies	Recipient	Designee
1	Research Center Fairchild Hiller Corporation Germantown, Maryland	Ralph Hall
1	Republic Aviation Corporation Fairchild Hiller Corporation Farmingdale, Long Island, New York	Library
1	General Dynamics, Convair Division Library & Information Services (128-00) P. O. Box 1128 San Diego, California 92112	Frank Dore
1	Missile and Space Systems Center General Electric Company Valley Forge Space Technology Center P. O. Box 8555 Philadelphia, Pennsylvania	F. Mezger F. E. Schultz
1	Grumman Aircraft Engineering Corporation Bethpage, Long Island, New York 11714	Joseph Gavin
1	Hughes Aircraft Company Aerospace Group Centinela and Teale Streets Culver City, California 90230	F. H. Meter V.P. and Div. Mgr. Research & Dev. Div.
1	Walter Rudde and Company, Inc. Aerospace Operations 567 Main Street Belleville, New Jersey	R. J. Hanville Dir. of Research Engr.
1	Arthur D. Little, Inc. 20 Acorn Park Cambridge, Massachusetts 02140	Library
1	Lockheed Missiles and Space Company Attn: Technical Information Center P. O. Box 504 Sunnyvale, California 94088	J. Guill

Copies	Recipient	Designee
1	Lockheed Propulsion Company P. O. Box 111 Redlands, California 92374	Library
1	The Marquardt Corporation 16555 Saticoy Street Van Nuys, California 91409	Library
1	Baltimore Division Martin Marietta Corporation Baltimore, Maryland 21203	John Calathes (3214)
1	Denver Division Martin Marietta Corporation P. O. Box 179 Denver, Colorado 80201	Dr. Morgenthaler A. J. Kullas
1	Astropower Laboratory McDonnell Douglas Astronautics Co. 2121 Campus Drive Newport Beach, California 92663	Dr. George Moe Director, Research
1	Missile and Space Systems Division McDonnell Douglas Astronautics Co. 3000 Ocean Park Boulevard Santa Monica, California 90406	Mr. R. W. Hallet Chief Engineer Adv. Space Tech.
1	Space & Information Systems Division North American Rockwell 12214 Lakewood Boulevard Downey, California 90241	Library
1	Aeronutronic Division Philco Corporation Ford Road Newport Beach, California 92663	D. A. Garrison
1	Astro-Electronics Division Radio Corporation of America Princeton, New Jersey 08540	Y. Brill

Copies	Recipient	Designee
1	Rocket Research Corporation 11441 Willow Road Redmond, Washington 98057	Foy McCullough, Jr.
1	Sundstrand Aviation 2421 11th Street Rockford, Illinois 61101	R. W. Reynolds
1	Standford Research Institute 333 Ravenswood Avenue Menlo Park, California 94025	Dr. Gerald Marksmen
1	TRW Systems Group TRW Incorporated One Space Park Redondo Beach, California 90278	G. W. Elverum
1	Thiokol Chemical Corporation Aerospace Services Elkton Division Bristol, Pennsylvania	Library
1	Research Laboratories United Aircraft Corporation 400 Main Street East Hartford, Connecticut 06108	Erle Martin
1	Hamilton Standard Division United Aircraft Corporation Windsor Locks, Connecticut 06096	R. Hatch
1	United Technology Center 587 Methilda Avenue P. O. Box 358 Sunnyvale, California 94088	Dr. David Altman
1	Republic Aviation Corporation Farmingdale, Long Island, New York	Dr. William O'Donnell
1	Space General Corporation 9200 East Flair Avenue El Monte, California 91734	C. E. Roth

Copies	Recipient	Designee
1	Thiokol Chemical Corporation Huntsville Division Huntsville, Alabama	John Goodloe
1	Calmec Manufacturing Corporation 5825 District Boulevard Los Angeles, California 90022	Library
1	Carleton Controls Corporation East Aurora, New York 14052	Library
1	J. C. Carter Company 671 W. Seventeenth Street Costa Mesa, California 92626	Library
1	Holex Incorporated 2751 San Juan Road Hollister, California 95023	Library
1	Parker Aircraft 5827 W. Century Boulevard Los Angeles, California 90009	Library
1	Pelmec Division Quantic Industries, Inc. 1011 Commercial Street San Carlos, California	Library
1	Pyronetics, Inc. 10025 Shoemaker Avenue Santa Fe Springs, California 90670	Library
1	Stratos Western Division of Fairchild-Hiller Corp. 1800 Rosecrans Boulevard Manhattan Beach, California	Library
1	Solar Division International Harvester Company 2200 Pacific Avenue San Diego, California	Library

Copies	Recipient	Designee
1	Vacco Valve Company 10350 Vacco Street South El Monte, California	Library
1	Valcor Engineering Corporation 365 Carnegie Avenue Kenilworth, New Jersey 07033	Library
1	Vickers, Inc. Division of Sperry Rand Corporation 2160 E. Imperial Highway El Segundo, California	Library
1	Whittaker Corporation 9601 Canoga Avenue Chatsworth, California 91311	Library
1	Wintec Corporation 343 Glasgow Inglewood, California	Library
1	McDonnell Douglas Astronautics Company P. O. Box 516 St. Louis, Missouri 63166 Attn: Mr. Shefman L. Hislop Director of Booster/Orbiter Integration	X
1	CCSD Michoud Operation P. O. Box 29200 New Orleans, Louisiana 70129 Attn: Mr. C. E. Tharrott, Dept. 2760	X
1	Grumman Aerospace Corporation Plant 25 - Space Shuttle Bethpage, L.I., New York 11714 Attn: Mr. Fred Raymer	X
1	Lockheed Missile and Space Company P. O. Box 504 Sunnyvale, California 94088 Attn: Mr. John Lloyd, Manager, Alternate Space Shuttle Concept Study, Dept. G1-51-Bldg. 538	X

Copies	Recipient	Designee
	Space Division North American Rockwell Corporation 12214 Lakewood Blvd. Downey, California 90241	
1	Attn: Mr. Joe Monroe	X
	The Boeing Company P. O. Box 1470 Huntsville, Alabama 35807	
1	Attn: Maxie Brown (Space Shuttle)	X

DOCUMENT CONTROL DATA - R & D

(Security classification of title, body of abstract and indexing annotation must be entered when the overall report is classified)

1. ORIGINATING ACTIVITY *(Corporate author)*	2a. REPORT SECURITY CLASSIFICATION
ROCKETDYNE a division of North American Rockwell Corporation 6633 Canoga Avenue, Canoga Park, California 91304	Unclassified
	2b. GROUP

3. REPORT TITLE

TITANIUM PUMP IMPELLER TESTING, FINAL REPORT

4. DESCRIPTIVE NOTES *(Type of report and inclusive dates)*

Final Report

5. AUTHOR(S) *(First name, middle initial, last name)*

James E. Wolf

6. REPORT DATE	7a. TOTAL NO. OF PAGES	7b. NO. OF REFS
1971	38	

8a. CONTRACT OR GRANT NO. NAS8-25060	9a. ORIGINATOR'S REPORT NUMBER(S) TMR 0115-3141
b. PROJECT NO.	
c.	9b. OTHER REPORT NO(S) *(Any other numbers that may be assigned this report)*
d.	

10. DISTRIBUTION STATEMENT

11. SUPPLEMENTARY NOTES	12. SPONSORING MILITARY ACTIVITY

13. ABSTRACT

This report describes the Ceramic Stresscoat burst and pump testing of two shrouded, diffusion-bonded titanium pump impellers. The Stresscoat test showed a significant decrease in centrifugal stress in relation to a geometrically similar machined impeller. The burst test demonstrated a higher tip speed at failure than the similar machined impeller in spite of an area of poor bonding, and the liquid hydrogen performance testing demonstrated the practicality of the diffusion bonding process to fabricate shrouded titanium impellers whose hydrodynamic design is not restricted by current machining methods.

DD FORM 1473
I NOV 65

14. KEY WORDS	LINK A		LINK B		LINK C	
	ROLE	WT	ROLE	WT	ROLE	WT
Ceramic Stresscoat						
Diffusion-bonded						
Shrouded						
Centrifugal stress						
Burst test						
Hydrodynamic design						
Elastic modules						
Statiflux						
H-Q characteristics						
Mismatch						